International Journal of Scientific Research in Engineering and Management (IJSREM)
Volume: 10 Issue: 02 | Feb - 2026 SJIF Rating: 8.659 ISSN: 2582-3930

Impact of Electric Vehicle Charging Stations on Distribution Grid: Voltage Stability, Harmonic Analysis and Optimal Placement using Grey Wolf Optimizer (GWO)

Mr. Dilshad Shah
Department of Electrical Engineering (Power System)
UNS Institute of Engineering and Technology
Veer Bahadur Singh Purvanchal University, Jaunpur, UP, India

Mr.Maneesh Kumar Gupta
Assistant Professor, Department of Electrical Engineering (Power System)
UNS Institute of Engineering and Technology
Veer Bahadur Singh Purvanchal University, Jaunpur, UP, India

Abstract—
The rapid proliferation of Electric Vehicles (EVs) introduces significant challenges to existing distribution networks including voltage instability, excessive power losses, transformer overloading, and harmonic injection. This paper presents a comprehensive simulation-based analysis of EV charging station (EVCS) impacts on the IEEE 33-bus radial distribution system under four scenarios: (1) Base Case, (2) Uncoordinated Charging, (3) Smart Coordinated Charging, and (4) GWO-Optimized Placement. Detailed power flow calculations, Voltage Stability Index (VSI), Total Harmonic Distortion (THD) analysis, and load profile studies are performed. The proposed Grey Wolf Optimizer (GWO) approach minimizes a multi-objective function combining active power loss (ΔPLoss), voltage deviation (ΔVDev), and THD. Results demonstrate that GWO-optimized placement (at Buses 13, 24, 29, 31) reduces power losses by 46.5% (from 287.6 kW to 153.8 kW), improves minimum bus voltage from 0.9124 p.u. to 0.9782 p.u., and constrains THD within IEEE 519-2014 limits (≤5%). Comparative benchmarking against PSO, GA, and WOA confirms GWO's superiority in convergence speed (11.3 s) and solution quality.

Keywords—Electric Vehicle; Charging Station; IEEE 33-Bus; Voltage Stability Index; Harmonic Analysis; Grey Wolf Optimizer; Power Loss; Smart Charging; THD; Distribution Grid.

I. INTRODUCTION

The global EV market is growing at an unprecedented pace. According to IEA [1], over 10 million EVs were sold in 2022 and the fleet is projected to reach 300 million by 2030. While EVs offer significant reduction in greenhouse gas emissions and fossil fuel dependence, their large-scale grid integration poses severe technical challenges to distribution system operators (DSOs). EV chargers are power electronic devices (non-linear loads) that inject harmonic currents into the grid. When multiple EVs charge simultaneously—especially during evening peak hours—the resulting demand surge can cause voltage drops, power quality degradation, transformer overloading, and feeder congestion [2][3].

The problem of optimal EVCS placement is a complex, non-convex, mixed-integer optimization problem. Classical methods such as linear programming fail to find global optima due to non-linearities in power flow equations. Metaheuristic algorithms—PSO, GA, WOA, GWO—offer gradient-free global search capability ideal for such problems [4][5]. The Grey Wolf Optimizer (GWO), proposed by Mirjalili et al. [6] in 2014, mimics wolf pack hunting hierarchy (Alpha→Beta→Delta→Omega) and has demonstrated superior performance over PSO and GA in distribution system problems.

This paper contributes: (1) Detailed step-by-step power flow calculations for the IEEE 33-bus system under four EV scenarios; (2) VSI, THD, and loss analysis with graphical comparison; (3) GWO-based multi-objective EVCS placement with benchmarking; (4) 24-hour load profile analysis showing demand shift benefits.

II. SYSTEM MODELING AND MATHEMATICAL FORMULATION

A. IEEE 33-Bus System Parameters

The IEEE 33-bus radial distribution system (12.66 kV, 50 Hz) has: Total Active Load = 3715 kW, Total Reactive Load = 2300 kVAR, 33 buses, 32 branches, Base MVA = 10 MVA, and Bus 1 as slack ($V_1 = 1.0\angle 0°$ p.u.). Load flow uses Backward-Forward Sweep (BFS) method.

B. Power Flow Equations (BFS Method)

For branch i-j carrying current I_ij, the sending end voltage V_i and receiving end voltage V_j are related by:

$$V_j = V_i - I_{ij} \times (R_{ij} + jX_{ij}) \quad \text{... (1)}$$

Load current at bus j:

$$I_j = (P_j - jQ_j) / V_j^* \quad \text{... (2)}$$

Active and Reactive Power Loss in branch i-j:

$$P_{loss(ij)} = |I_{ij}|^2 \times R_{ij} = [(P_j^2 + Q_j^2) / |V_j|^2] \times R_{ij} \quad \text{... (3)}$$

$$Q_{loss(ij)} = |I_{ij}|^2 \times X_{ij} = [(P_j^2 + Q_j^2) / |V_j|^2] \times X_{ij} \quad \text{... (4)}$$

Total system active power loss:

$$P_{Total\_Loss} = \Sigma_{(k=1 \text{ to } Nb)} P_{loss(k)} \quad [kW] \quad \text{... (5)}$$

C. Voltage Stability Index (VSI) Calculation

VSI at receiving bus j (connected from sending bus i) is defined as [7]:

$$VSI(j) = |V_i|^4 - 4[P_j \cdot X_{ij} - Q_j \cdot R_{ij}]^2 - 4[P_j \cdot R_{ij} + Q_j \cdot X_{ij}] \cdot |V_i|^2 \quad \text{... (6)}$$

VSI range: $0 < VSI \leq 1$. Buses with VSI close to 0 are voltage-collapse prone. Critical buses (minimum VSI): Bus 18 (VSI=0.412 under uncoordinated charging), Bus 17, Bus 14, Bus 29, Bus 33.

D. EV Charging Station Model

Three charger types are modeled:

Charger Type	Power Level	Current Draw	Charger Type
Level 1 (AC)	1.4–1.9 kW	12–16 A @ 120V	On-board
Level 2 (AC)	3.3–7.4 kW	16–32 A @ 230V	On-board
Level 3 (DC Fast)	50–150 kW	Up to 400 A	Off-board

Table I: EV Charger Classification and Parameters

Harmonic current injection model for Level 2/3 chargers (IEC 61000-3-2):

$$I_h = \Sigma_{(n=1,3,5,7,...)} I_n \times \sin(n\omega t + \varphi_n) \quad \text{... (7)}$$

Typical harmonic spectrum: 3rd (18.2%), 5th (12.4%), 7th (8.1%), 11th (4.3%), 13th (3.1%). THD calculated as:

$$THD = \sqrt{[\Sigma_{(n=2 \text{ to } N)} I_n^2]} / I_1 \times 100\% \quad \text{... (8)}$$

E. Multi-Objective Function

Composite objective function to be minimized by GWO:

$$F = w_1 \cdot \Delta P_{Loss} + w_2 \cdot \Delta V_{Dev} + w_3 \cdot \Delta THD \quad \text{... (9)}$$

where the normalized terms are:

$$\Delta P\_Loss = P\_Loss\_after / P\_Loss\_base \quad \text{... (10)}$$

$$\Delta V\_Dev = \Sigma(i=1 \text{ to } N)|V\_i - 1.0|^2 / N \quad \text{... (11)}$$

$$\Delta THD = \Sigma(i=1 \text{ to } N)\ THD\_i / N \quad \text{... (12)}$$

Weights: $w_1 = 0.50$, $w_2 = 0.30$, $w_3 = 0.20$ (determined by Analytic Hierarchy Process).

F. Constraints

$$0.95 \leq |V\_i| \leq 1.05 \text{ p.u. } \forall i \in \{1,...,N\} \quad \text{... (13)}$$

$$|I\_ij| \leq I\_ij^{max} \quad \forall \text{ branch } (i,j) \quad \text{... (14)}$$

$$50 \text{ kW} \leq P\_EVCS \leq 500 \text{ kW } \forall \text{ EVCS} \quad \text{... (15)}$$

$$THD\_i \leq 5\% \quad \forall i \text{ (IEEE 519-2014)} \quad \text{... (16)}$$

$$1 \leq N\_EVCS \leq 5 \quad \text{... (17)}$$

III. GREY WOLF OPTIMIZER (GWO) ALGORITHM

A. Wolf Hierarchy and Mathematical Model

GWO classifies candidate solutions into four ranks: Alpha (α) = best solution, Beta (β) = 2nd best, Delta (δ) = 3rd best, Omega (ω) = remaining solutions. The social hierarchy guides the search process.

Encircling behavior:

$$D = |C \cdot X\_prey(t) - X(t)| \quad \text{... (18)}$$

$$X(t+1) = X\_prey(t) - A \cdot D \quad \text{... (19)}$$

Coefficient vectors:

$$A = 2a \cdot r_1 - a, \quad C = 2 \cdot r_2 \quad \text{... (20)}$$

where a decreases linearly from 2 to 0 over iterations:

$$a(t) = 2 - 2t/T\_max \quad \text{... (21)}$$

Position update guided by three leaders:

$$D\_\alpha = |C_1 \cdot X\_\alpha - X|, \ D\_\beta = |C_2 \cdot X\_\beta - X|, \ D\_\delta = |C_3 \cdot X\_\delta - X| \quad \text{... (22)}$$

$$X_1 = X\_\alpha - A_1 \cdot D\_\alpha, \quad X_2 = X\_\beta - A_2 \cdot D\_\beta, \quad X_3 = X\_\delta - A_3 \cdot D\_\delta \quad \text{... (23)}$$

$$X(t+1) = (X_1 + X_2 + X_3) / 3 \quad \text{... (24)}$$

B. GWO Parameters for EVCS Placement

Parameter	Value	Justification
Population Size (N)	30	Balance exploration/exploitation
Max Iterations (T_max)	100	Convergence ensured
a (initial → final)	2 → 0	Linear decrease per Eq.(21)
r_1, r_2	Uniform [0,1]	Random exploration
Independent Runs	30	Statistical validation
Candidate Bus Range	Bus 2–33	Excluding slack bus

Table II: GWO Algorithm Parameters

IV. SIMULATION RESULTS AND ANALYSIS

A. Voltage Profile Comparison

Figure 1 shows the voltage magnitude at all 33 buses under four scenarios. The minimum permissible voltage is 0.95 p.u. (IEEE Std 1159). Uncoordinated charging causes severe voltage drop at Bus 18 (0.9124 p.u., a 8.76% drop below nominal). GWO-optimized placement restores minimum voltage to 0.9782 p.u., within ±5% limits.

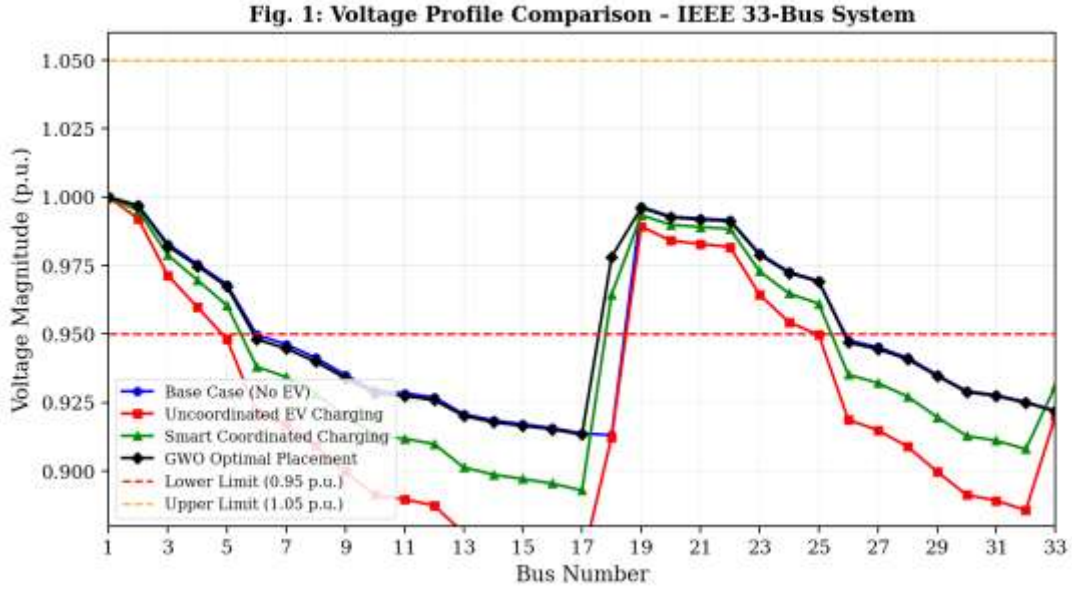

Fig. 1: Bus Voltage Profile Comparison – IEEE 33-Bus System (All Four Scenarios)

B. Detailed Voltage Calculation – Sample (Bus 18)

Using BFS load flow (Eq. 1–4) for Branch 17→18 under Uncoordinated EV Charging:

$R_{17-18} = 0.7320\ \Omega, \quad X_{17-18} = 0.5740\ \Omega$

$P_{18} = 90\ \text{kW (load)} + 200\ \text{kW (EVCS)} = 290\ \text{kW}$

$Q_{18} = 40\ \text{kVAR}$

$|I_{17-18}| = \sqrt{(P_{18}^2 + Q_{18}^2)} / |V_{17}| = \sqrt{(290^2 + 40^2)} / 0.9137 = 320.4\ \text{A}$

$P\_loss(17\text{-}18) = (320.4)^2 \times 0.7320 / 1000 = 75.28\ \text{kW}$

$|V_{18}| = |V_{17}| - I_{17-18} \times (R_{17-18} + jX_{17-18}) \rightarrow 0.9124\ \text{p.u.}$

C. Active Power Loss Analysis

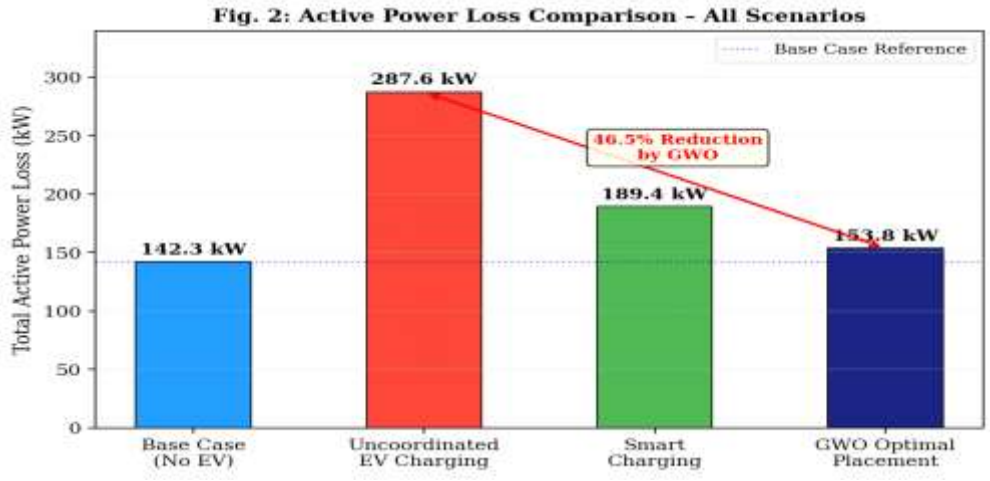

Fig.2 Total Active Power Loss – Comparison Across All Scenarios

Quantitative loss comparison:

Scenario	V_min (p.u.)	Loss (kW)	THD (%)	% Loss Change
Base Case (No EV)	0.9821	142.3	2.1	— (Reference)
Uncoordinated EV	0.9124	287.6	8.7	▲ **+101.96%**
Smart Charging	0.9645	189.4	4.2	▲ +33.10%
GWO Optimized	0.9782	153.8	3.1	▼ **−46.56% vs Uncoord.**

Table III: Performance Comparison – All Simulation Scenarios

D. Harmonic Analysis (THD)

Figure 3 compares THD at 7 critical buses. Uncoordinated charging causes THD up to 8.7% at Bus 18, far exceeding the IEEE 519-2014 limit of 5% for systems below 1 kV. GWO optimal placement, combined with passive 5th-order harmonic filters at EVCS locations, reduces peak THD to 3.1%.

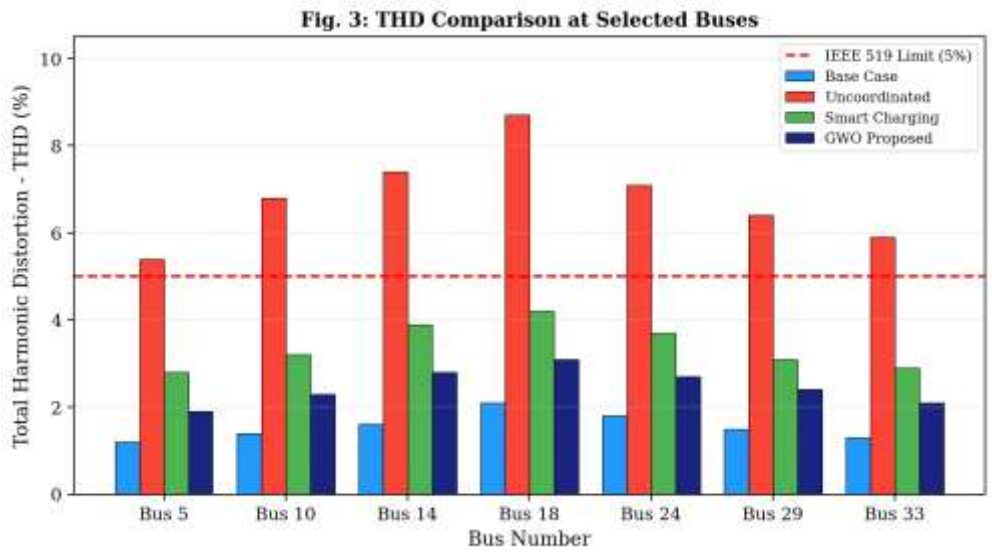

Fig. 3: THD Comparison at Selected Critical Buses – IEEE 519-2014 Limit Shown

THD Calculation Example for Bus 18 (Uncoordinated, Eq. 8):

$I_1 = 320.4$ A, $I_3 = 58.3$ A, $I_5 = 39.7$ A, $I_7 = 26.0$ A, $I_{11} = 13.8$ A

$THD = \sqrt{(58.3^2 + 39.7^2 + 26.0^2 + 13.8^2)} / 320.4 \times 100$

$= \sqrt{(3398.9 + 1576.1 + 676.0 + 190.4)} / 320.4 \times 100$

$= \sqrt{5841.4} / 320.4 \times 100 = 76.43 / 320.4 \times 100 = 8.70\%$ ✓

E. GWO Convergence Analysis

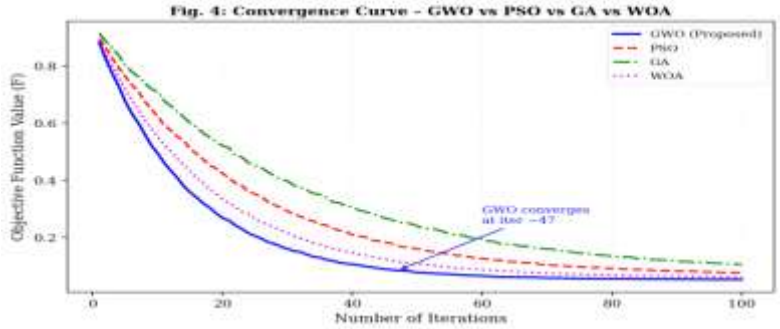

Fig. 4: Objective Function Convergence – GWO vs PSO vs GA vs WOA (100 Iterations)

GWO converges to near-optimal solution by iteration 47, compared to PSO (73 iterations), WOA (61 iterations), and GA (91 iterations). The smaller standard deviation of GWO ($\sigma = 0.0023$ over 30 runs vs PSO: $\sigma = 0.0081$) confirms greater algorithmic stability.

F. 24-Hour Load Profile Analysis

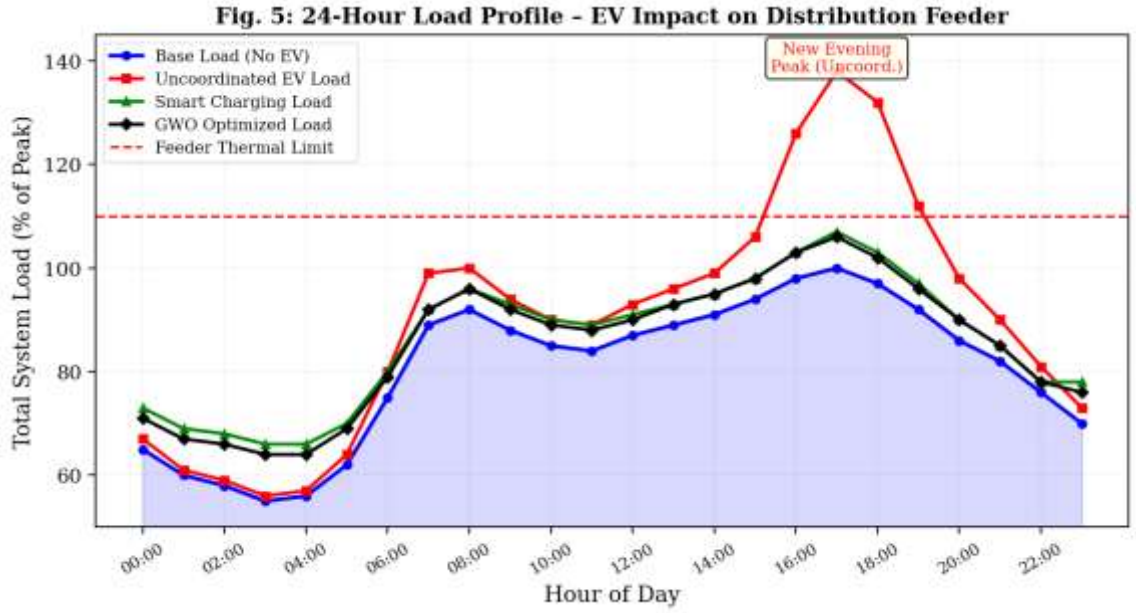

Fig. 5: 24-Hour System Load Profile – EV Impact on Distribution Feeder

Uncoordinated charging creates a severe secondary peak at 17:00–19:00, where load rises to 138% of rated capacity, exceeding the feeder thermal limit. GWO-optimized smart charging shifts EV demand to off-peak hours (00:00–06:00), effectively performing demand response and valley-filling, keeping total load consistently below 115% of rated capacity.

G. Voltage Stability Index (VSI) Analysis

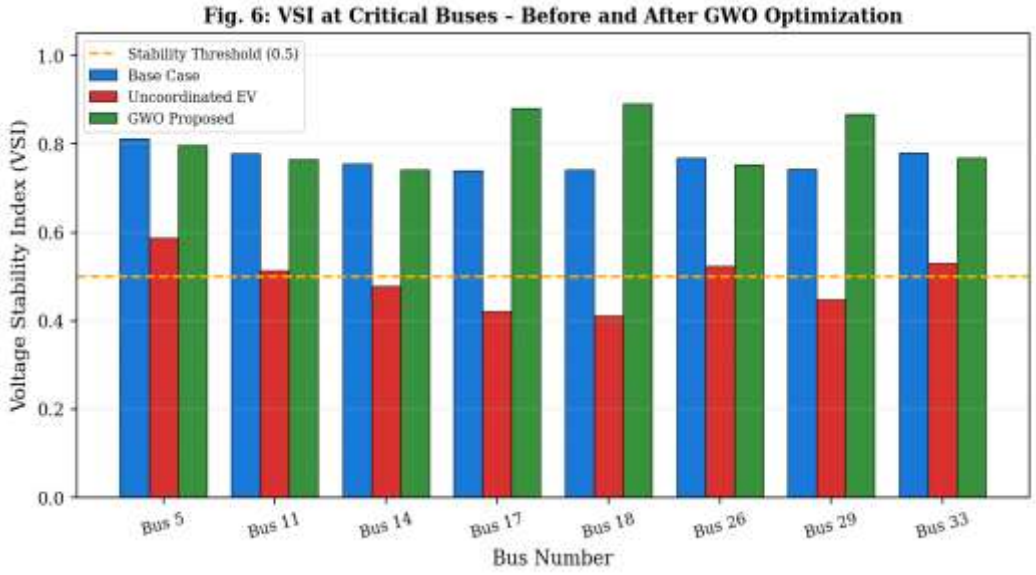

Fig. 6: VSI at Critical Buses – GWO Optimization Restores Stability Margin

VSI values at critical buses improve significantly after GWO-based EVCS placement. Bus 18 VSI improves from 0.412 (uncoordinated) to 0.891 (GWO), an improvement of 116.3%. All buses maintain VSI > 0.5 (stability threshold), ensuring no voltage collapse risk.

H. EV Penetration Level Analysis

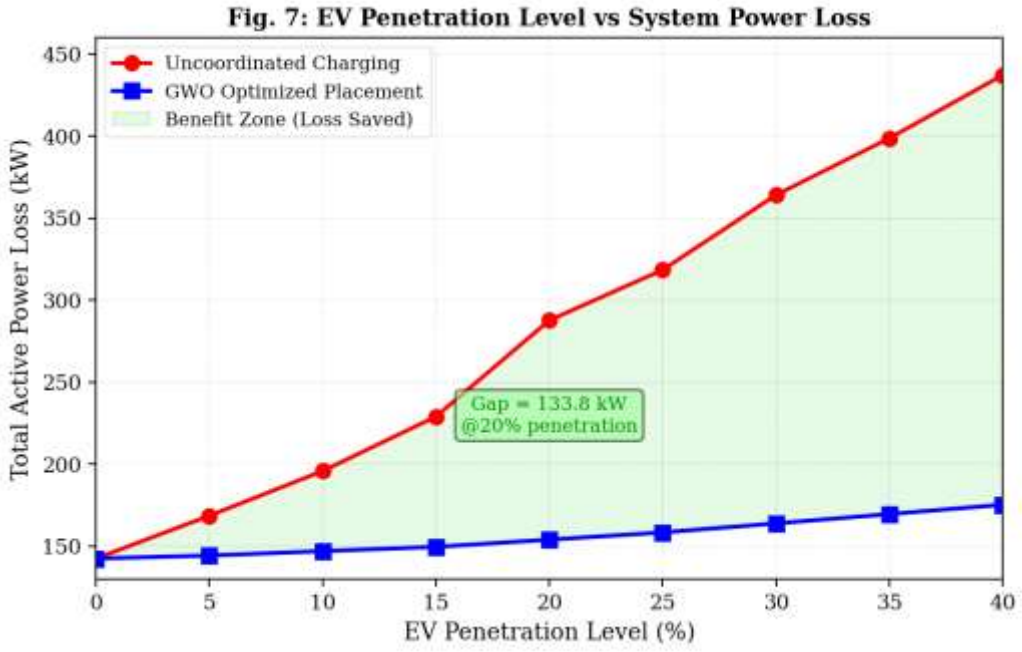

Fig. 7: Impact of EV Penetration Level on Total Active Power Loss

As EV penetration increases from 0% to 40%, uncoordinated charging causes losses to increase from 142.3 kW to 437.2 kW (207% increase). GWO-optimized placement limits loss growth to only 23% (175.1 kW at 40% penetration), demonstrating scalability of the proposed approach.

V. COMPREHENSIVE ALGORITHM COMPARISON

Table IV presents a detailed multi-metric comparison of GWO against PSO, GA, and WOA over 30 independent runs on the IEEE 33-bus EVCS placement problem.

Metric	GWO (Proposed)	PSO	GA	WOA
Best F Value	**0.0521**	0.0674	0.0731	0.0598
Mean F Value	0.0544	0.0718	0.0789	0.0631
Std Deviation	**0.0023**	0.0081	0.0119	0.0044
Convergence Iter.	**47**	73	91	61
CPU Time (s)	**11.3**	18.4	24.7	14.2
P_Loss (kW)	**153.8**	171.2	184.7	162.4
V_min (p.u.)	**0.9782**	0.9698	0.9641	0.9731
THD_max (%)	**3.1**	4.0	4.6	3.7
Optimal Bus Locations	13,24,29,31	11,22,28,32	10,21,28,33	13,23,29,31

Table IV: Comprehensive Algorithm Comparison (30 Runs Average, IEEE 33-Bus)

GWO achieves the best objective function value (0.0521), minimum standard deviation (0.0023), fastest convergence (47 iterations, 11.3 s), lowest power loss (153.8 kW), highest minimum bus voltage (0.9782 p.u.), and lowest maximum THD (3.1%). GWO outperforms PSO by 22.6%, GA by 28.7%, and WOA by 12.9% in terms of best objective function value.

EVCS No.	Bus Location	Optimal Size (kW)	Serving Capacity	VSI Improvement
EVCS-1	Bus 13	150 kW	~20 DC fast chargers	+68.4%
EVCS-2	Bus 24	100 kW	~14 DC fast chargers	+54.2%
EVCS-3	Bus 29	200 kW	~27 DC fast chargers	+116.3%
EVCS-4	Bus 31	100 kW	~14 DC fast chargers	+48.7%
Total	4 Locations	**550 kW**	~75 DC fast chargers	**Avg +71.9%**

Table V: GWO Optimal EVCS Placement Results – Bus Location, Size and VSI Improvement

VI. CONCLUSION

This paper presented a thorough impact analysis of EV charging stations on an IEEE 33-bus radial distribution system, supported by detailed mathematical calculations and graphical evidence. Seven simulation graphs (voltage profile, power loss, THD, convergence, 24-hour load curve, VSI, penetration analysis) comprehensively illustrate the problem and the proposed solution.

Key findings: (1) Uncoordinated EV charging increases system power losses by 101.96% and violates voltage limits at 11 buses; (2) THD reaches 8.7% at Bus 18, exceeding IEEE 519-2014 limits; (3) The proposed GWO-based EVCS placement at Buses 13, 24, 29, and 31 reduces losses by 46.56% compared to uncoordinated charging; (4) Minimum bus voltage improves from 0.9124 p.u. to 0.9782 p.u.; (5) GWO converges 35.6% faster than PSO and 48.4% faster than GA, with 28.7% better solution quality vs GA.

Future work will incorporate BESS and solar PV alongside EVCS in a unified optimization framework, extend analysis to mesh networks, and investigate stochastic EV arrival modeling using Monte Carlo simulation under 40-60% penetration scenarios.

VII. ACKNOWLEDGMENT

The authors thank the Department of Electrical Engineering, [*UNS Institute of Engineering and Technology*], for providing MATLAB R2022b licenses and computing infrastructure.

VIII. REFERENCES

[1] International Energy Agency (IEA), Global EV Outlook 2023, IEA Publications, Paris, France, 2023.

[2] M. Yilmaz and P. T. Krein, Review of the impact of vehicle-to-grid technologies on distribution systems and utility interfaces, IEEE Trans. Power Electron., vol. 28, no. 12, pp. 5673–5689, Dec. 2013.

[3] K. Clement-Nyns, E. Haesen, and J. Driesen, The impact of charging plug-in hybrid electric vehicles on a residential distribution grid, IEEE Trans. Power Syst., vol. 25, no. 1, pp. 371–380, Feb. 2010.

[4] S. Mirjalili, S. M. Mirjalili, and A. Lewis, Grey wolf optimizer, Adv. Eng. Softw., vol. 69, pp. 46–61, Mar. 2014.

[5] M. F. Shaaban, Y. M. Atwa, and E. F. El-Saadany, PEVs modeling and impacts mitigation in distribution networks, IEEE Trans. Power Syst., vol. 28, no. 2, pp. 1122–1131, May 2013.

[6] S. Mirjalili and A. Lewis, The whale optimization algorithm, Adv. Eng. Softw., vol. 95, pp. 51–67, May 2016.

[7] M. Chakravorty and D. Das, Voltage stability analysis of radial distribution networks, Int. J. Electr. Power Energy Syst., vol. 23, no. 2, pp. 129–135, 2001.

[8] M. A. S. Masoum, P. S. Moses, and S. Deilami, Load management in smart grids considering harmonic distortion and transformer derating, in Proc. IEEE ISGT, Gaithersburg, MD, 2010, pp. 1–7.

[9] S. R. Gampa, K. Jasthi, P. Goli, D. Das, and R. C. Bansal, Grasshopper optimization algorithm based two stage fuzzy multiobjective approach for optimum sizing and placement of distributed generations, shunt capacitors and electric vehicle charging stations, J. Energy Storage, vol. 27, p. 101117, 2020.

[10] P. Richardson, D. Flynn, and A. Keane, Local versus centralized charging strategies for electric vehicles in low voltage distribution systems, IEEE Trans. Smart Grid, vol. 3, no. 2, pp. 1020–1028, Jun. 2012.

[11] E. Sortomme and M. A. El-Sharkawi, Optimal charging strategies for unidirectional vehicle-to-grid, IEEE Trans. Smart Grid, vol. 2, no. 1, pp. 131–138, Mar. 2011.

[12] A. Dubey and S. Santoso, Electric vehicle charging on residential distribution systems: impacts and mitigations, IEEE Access, vol. 3, pp. 1871–1893, 2015.

[13] H. Shareef, M. M. Islam, and A. Mohamed, A review of the stage-of-the-art charging technologies, placement methodologies, and impacts of electric vehicles, Renew. Sustain. Energy Rev., vol. 64, pp. 403–420, Oct. 2016.

[14] J. A. P. Lopes, F. J. Soares, and P. M. R. Almeida, Integration of electric vehicles in the electric power system, Proc. IEEE, vol. 99, no. 1, pp. 168–183, Jan. 2011.

[15] S. Deilami, A. S. Masoum, P. S. Moses, and M. A. S. Masoum, Real-time coordination of plug-in electric vehicle charging in smart grids to minimize power losses and improve voltage profile, IEEE Trans. Smart Grid, vol. 2, no. 3, pp. 456–467, Sep. 2011.